PARTICLE SWARM OPTIMIZATION FOR BLURRED CONTOUR RETRIEVAL

Julien Marot and Salah Bourennane

Institut Fresnel, Ecole Centrale Marseille, Aix Marseille Universite
D. U. de Saint-Jérôme, 13397, Marseille, France
phone: + (33) 4 91 28 82 02, email: julien.marot@fresnel.fr
web: www.fresnel.fr/perso/marot

ABSTRACT

This paper concentrates on the estimation of linear and circular blurred contours in an image. To solve this problem, we start from recently investigated signal models, derived through the association of an array of virtual sensors and the image. The array is linear when linear blurred contours are expected, and circular when circular blurred contours are expected. For the first time in this paper, we propose a common array processing model for both types of contours, which makes their retrieval closer to each other. We propose a common criterion to minimize for the estimation of the contour parameters, and justify the usage of particle swarm optimization for its minimization. An application to fire characterization exemplifies our method.

Index Terms— Blurred contour, Sensor Array, Optimization, Fire surveillance

1. INTRODUCTION

Characterizing contours, regions or objects which are not simply defined by a one-pixel wide contour attracted recently much interest. Firstly, region-based segmentation such as in [1], where thick boundaries are delimitated through an inner and an outer part; secondly contour-based segmentation [2, 3] were proposed. Getting inspired from the seminal work proposed in [2], where active contours seek for low-contrast boundaries, Fang and Chan, in [3], incorporate a shape prior model into geodesic active contours to detect low contrast boundaries despite the presence of occluded objects. These methods always provide results as one-pixel wide contours.

Relation to prior work in the field

Two papers show the interest of array processing signal models and methods for the characterization of blurred contours: they shed light on linear [4] and circular [5] blurred contours. No common frame was proposed for both types of contours, and only a local Gradient optimization has been proposed to characterize circles yet.

The first contribution of this paper consists in relating linear and circular blurred contour retrieval: we propose a common signal model in Section 2. To estimate the contour parame-

ters, we derive a criterion involving the signal generated from the image and this common signal model. For the first time, we take into account the nonlinear dependence of the minimized criterion versus the expected parameters: we show in Section 3 that particle swarm optimization (PSO) is adequate to minimize the proposed criterion. In Section 4, an application to wild fire surveillance illustrates the proposed method.

2. A COMMON SIGNAL MODEL FOR BLURRED CONTOURS

In this section, we provide the models that we adopt for the image and contours. We show that, if we restrict the shape of the expected blurred contours to linear or circular, we get an exponential signal model when the appropriate signal generation method is adopted.

2.1. Image and contour models

Let $I(l, m)$ be an $N \times N$ recorded image (see Figure 1(a) or Figure 1(b)). We assume that $I(l, m)$ is compound of blurred linear or circular contours, and an additive uniformly distributed noise, whose gray level values follow a Gaussian distribution. A linear-like contour is supposed to have main orientation θ. We define its center offset x_0 as the distance between the top left corner of the image and the pixel with maximum gray level value $I_{\max}$ in the first row (see Figure 1(a)). what we call the mid contour of a blurred line or circle is the one-pixel wide contour which best fits this contour. The spread of the contour is characterized by the parameter σ, and we define the parameter G such that $I_{\max} = \frac{G}{\sqrt{2\pi}\sigma}$. When d blurred linear contours are present, they are defined by the set of parameters $\{\theta_k, x_{0k}, \sigma_k, k = 1, \ldots, d\}$. A circular-like contour is supposed to have center coordinates $\{l_c; m_c\}$ (see Figure 1(b)). The pixels with value $\frac{G}{\sqrt{2\pi}\sigma}$ compound a circle with center coordinates $\{l_c; m_c\}$ and radius r. When concentric circles are present, their radius values are $\{r_k, k = 1, \ldots, d\}$. A blurred linear contour has width $2X_f$, and a blurred circular-like contour has width $2r_f$. We model
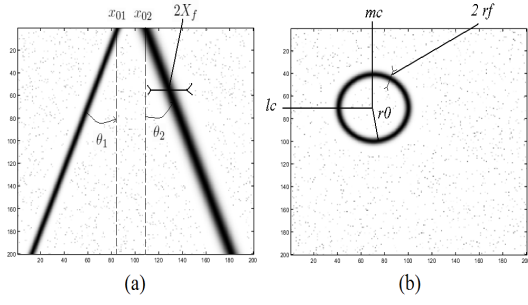
Fig. 1. Contour models: (a) blurred contours characterized by main orientations θ_1, θ_2, offsets x_{01} and x_{02}, and width $2X_f$; (b) blurred circular contour characterized by center coordinates $\{l_c; m_c\}$, radius r, and width $2r_f$.

the contour grey level values as follows:

$$I(l,m) = \frac{G}{\sqrt{2\pi}\sigma}e^{-\frac{x^2}{2\sigma^2}}, \tag{1}$$

where $x = m - (x_0 - (l-1)tan(\theta))$; and:

$$I(l,m) = \frac{G}{\sqrt{2\pi}\sigma}e^{-\frac{(\sqrt{(l-l_c)^2+(m-m_c)^2}-r)^2}{2\sigma^2}} \tag{2}$$

We check that in (1) and (2), $\frac{G}{\sqrt{2\pi}\sigma}$ is the maximum gray level value.

2.2. Signal generation and signal models

To generate a signal out of the image, an array of sensors, also called antenna, is associated with the image. The array
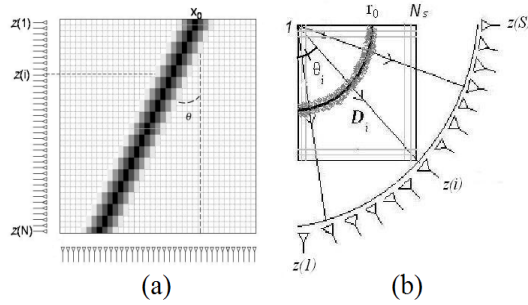

Fig. 2. Signal generation: (a) linear antenna for the generation of signal components $z(1)$, $z(2)$, ..., $z(N)$ on left and bottom sides, blurred linear-like contour with orientation θ and offset x_0; (b) sub-image of size $N_S \times N_S$ circular antenna [7] for the generation of signal components $z(1)$, $z(2)$, ..., $z(S)$ with i^{th} sensor at angular position θ_i and associated direction of generation D_i, blurred quarter of circle

is either linear (see Figure 2(a)) or circular (see Figure 2(b)). Signal generation on linear antenna was first proposed in [6].

Each signal component reads:

$$z(i) = \sum_{m=1}^{N} I(i,m)\,e^{-j\mu m}, \; (i=1,\dots,N), \tag{3}$$

where $j = \sqrt{-1}$, and μ is an *a priori* set propagation parameter. The signal components form the following signal vector: $\mathbf{z} = [z(1), z(2), \dots, z(N)]^T$.

Signal generation on circular antenna was first proposed in [7]. Each signal component reads:

$$z(i) = \sum_{\substack{l=1 \\ (l,m)\in D_i}}^{N_s} \sum_{m=1}^{N_s} I(l,m)e^{-j\mu\sqrt{l^2+m^2}}, \tag{4}$$

where N_s is the size of the considered quarter of image (see Fig. 2(b)). The signal components form the following signal vector: $\mathbf{z} = [z(1), z(2), \dots, z(S)]^T$. In [4] and [5], these signal generation schemes were applied to images containing linear (resp. circular) blurred contours. Firstly, we consider the linear contour case [4]: d blurred contours are expected, with orientations θ_k, offsets x_{0k}, and spread parameters σ_k ($k = 1, \dots, d$). Uniformly distributed noise pixels, whose gray level values follow a Gaussian distribution, impair the image.

The signal generation scheme of (3) yields:

$$z(i) = \sum_{k=1}^{d} s(x_{0k}, \sigma_k)c_i(\theta_k) + n(i) \tag{5}$$

where $c_i(\theta_k) = e^{j\mu(i-1)\tan(\theta_k)}$.
and for $k = 1, \cdots, d$:

$s(k) = \frac{G}{\sqrt{2\pi}\sigma}e^{-j\mu x_{0k}}\sum_{x=-X_f}^{X_f}e^{-j\mu x}e^{-\frac{x^2}{2\sigma_k^2}}$, which can be approximated as a Riemann integral (see [4] and [5]) and finally yield:

$s(k) = Ge^{-j\mu x_{0k}}e^{-\frac{\mu^2\sigma_k^2}{2}}$.

Secondly, we consider the case of d concentric circular contours, in a noisy environment. We have shown in [5] that we get a linear phase signal if we set $\mu = \alpha(i-1)$, where α is a constant. The signal generation scheme (4) yields:

$$z(i) = G\sum_{k=1}^{d} e^{-j\alpha(i-1)r_k}e^{-\frac{\sigma_k^2\alpha^2(i-1)^2}{2}} + n(i). \tag{6}$$

This can be expressed as:

$$z(i) = \sum_{k=1}^{d} s_k c_i(r_k, \sigma_k) + n(i) \tag{7}$$

where:
$c_i(r_k, \sigma_k) = Ge^{-\frac{\sigma_k^2\alpha^2(i-1)^2}{2}}e^{-j\alpha(i-1)r_k}$;
$s_k = 1, k = 1, \cdots, d$.
We notice that the signal models for (5) and (7) are similar. In a matrix form, we get:

$$\mathbf{z} = \mathbf{C}(\iota)\mathbf{s}(\kappa) + \mathbf{n} \tag{8}$$

In the case of blurred lines, ι stands for the set of parameters $\{\theta_1, \ldots, \theta_d\}$ and κ stands for the couples of parameters $\{(x_{01}, \sigma_1), \ldots, (x_{0d}, \sigma_d)\}$; and in the case of blurred circles, ι stands for couples of parameters $\{(r_1, \sigma_1), \ldots, (r_d, \sigma_d)\}$ and contains all the paramaters of the signal model. The source vector and steering matrix are defined by $\mathbf{s} = [s(\kappa_1), \ldots, s(\kappa_d)]^T$ and $\mathbf{C}(\iota) = [\mathbf{c}(\iota_1), \ldots, \mathbf{c}(\iota_d)]^T$, with, $\forall\, k$, $\mathbf{c}(\iota_k) = [c_1(\iota_k), \ldots, c_{NS}(\iota_k)]^T$. The signal and noise vectors are $\mathbf{z} = [z(1), \ldots, z(NS)]^T$ and $\mathbf{n} = [n(1), \ldots, n(NS)]^T$, with either $NS = N$ when lines are expected or $NS = S$ when circles are expected. With this unified signal model, we provide in a synthetic form a common formalism involving PSO to estimate the parameters of either blurred lines or blurred circles. Once the category of expected contour is known, the estimation method holds for linear and circular contours.

3. PARTICLE SWARM OPTIMIZATION

In [4,5], subspace-based algorithm are used to compute an estimate of either $\{\theta_k, x_{0k}\}$, $k = 1, \ldots, d$ for linear contours, or $\{r_k\}$, $k = 1, \ldots, d$ for circular contours (see [4, 5]), but an approximation is made: the source vector is supposed not to vary as a function of the sensor index, which may yield a bias on the estimated parameters.

In this paper, we propose for the first time a common framework to estimate all contour parameters, ι and κ, that is either in a $3d$ dimensional space for lines, or in $2d$ dimensional space for circles, without any approximation. Firstly, we detail the criterion which is minimized for this purpose. Secondly, we justify the use of particle swarm optimization [10] as an optimization method to perform the criterion minimization.

We propose to minimize a scalar criterion to estimate the contour parameters:
we set $J(\iota, \kappa) = ||\mathbf{z} - \mathbf{C}(\iota)\mathbf{s}(\kappa)||^2$, where $||.||$ represents the Frobenius norm, and $\mathbf{z}$ is the signal generated from the image. We wish to solve:

$$\hat{\iota}, \hat{\kappa} = \underset{\iota, \kappa}{argmin}(J(\iota, \kappa)) \qquad (9)$$

It is rather complex to minimize the criterion J as it is a nonlinear function of the parameters in vectors ι and κ. Hence the need for an adequate optimization method, which must be global, and fast.

The criterion J does not fulfill the requirements of the DIRECT optimization method [9], as it is no Lipschitzian function of ι and κ. In [5], we proposed a Gradient scheme restricted to circular contours. It may converge to a local minimum of the criterion minimized for this purpose. The Nelder-Mead Simplex Method [8] could be adapted: it is meant to minimize a scalar-valued nonlinear function of several real variables, without any derivative information. However, as specified in [8], the global convergence of the

Nelder-Mead method is ensured only in a one-dimensional problem, if some conditions about the parameters involved in the method are respected. For all these reasons, we choose to adapt particle swarm optimization [10]. Particle Swarm Optimization [10] and Genetic Algorithm are two popular methods for their advantages such as gradient-free and ability to find global optima. The basic PSO algorithm consists, for the current iteration number it, of the velocity:

$$\mathbf{v}_q^{\iota,\kappa}(\text{it} + 1) = W\, \mathbf{v}_q^{\iota,\kappa}(\text{it}) + \gamma_{1q}\, r1_q(\mathbf{p}_q^{\iota,\kappa} - \mathbf{y}_q^{\iota,\kappa}(\text{it}))$$

$$... + \gamma_{2q}\, r2_q(\mathbf{G}^{\iota,\kappa} - \mathbf{y}_q^{\iota,\kappa}(\text{it})) \qquad (10)$$

and of the position:

$$\mathbf{y}_q^{\iota,\kappa}(\text{it} + 1) = \mathbf{y}_q^{\iota,\kappa}(\text{it}) + \mathbf{v}_q^{\iota,\kappa}(\text{it} + 1) \qquad (11)$$

In (10) and (11), $\mathbf{v}_q^{\iota,\kappa}(\text{it})$ is the velocity of particle q at iteration it in a $2d$ or $3d$-dimensional space, depending on the type of expected contour, W is the inertia weight, γ_{1q} and γ_{2q} are the acceleration constants encouraging a local and a global search respectively, $r1_q$ and $r2_q$ are random numbers between 0 and 1, applied to the qth particle, $\mathbf{p}_q^{\iota,\kappa}$ is the best position found for particle q, $\mathbf{G}^{\iota,\kappa}$ is the best position found over the whole group, and $\mathbf{y}_q^{\iota,\kappa}(\text{it})$ is the current position of particle q at iteration it. A large inertia weight (W) facilitates a global search while a small inertia weight facilitates a local search. We look forward to encourage a global search for the first iterations, and a local search for the last iterations. Hence, we fix an initial value W_{Init} and a final value W_{Final} for the weighting coefficient. At the iteration it, the weighting coefficient is computed as:
$W = W_{Init} - \frac{(W_{Init} - W_{Final}) * \text{it}}{\text{maxit}}$, where maxit is the final iteration number. When this last iteration number is attained, the position vector $\mathbf{y}^{\iota,\kappa}(\text{maxit})$ contains the final estimation of all parameters in $\hat{\iota}$ and $\hat{\kappa}$, which characterize entierely the expected contours.

4. RESULTS

We consider images of size $N \times N$. In the first example, a hand-made image with $N = 400$ is processed; in the second example, a real-world image with $N = 200$ is processed. Their grey level values are encoded on 8 bits. To run the PSO algorithm, the maximum number of iterations maxit is 2000; the swarm size is 25. By increasing the population size, we enable the PSO to search more points and thereby we can obtain a better result. However, the larger the population size is, the longer the PSO takes to compute each iteration. The acceleration constants γ_{1i} and γ_{2i} are set to 2 and 3 respectively; the initial and final values of W are set to 0.9 and 0.4. We initialize the parameters in ι and κ as random values. To draw the result images, we fix the contour half width to $r_f = 1.5\sigma$. Aside, the gray level values are considered as negligible.

4.1. Linear blurred contours

We assume the presence of $d = 2$ linear blurred contours. To fix the constant propagation parameter μ, we proceed heuristically but still avoiding any phase indeterminacy in the terms $c_i(\theta_k)$ and $s(k)$ of (5). The value to $\mu = 0.1$, for instance, is convenient. On the condition that we adopt this order of magnitude, the parameter estimation method is robust to variations in the propagation parameter value. Figure 3 exemplifies the case where the spread parameters are $\sigma_1 = 1$ and $\sigma_2 = 8$ respectively, the offsets of two blurred contours $x_{01} = 170$ and $x_{02} = 200$, and the main orientation of two contours are $\theta_1 = 18°$ and $\theta_2 = -18°$. Orientation values are estimated as $18°$ and $-18°$. Offset values are estimated as 211 and 200. The spread parameters are estimated as 1 and 9. The observed bias may come from the Riemann integral approximation (see subsection 2.2). The proposed method lasts 2.5 sec.
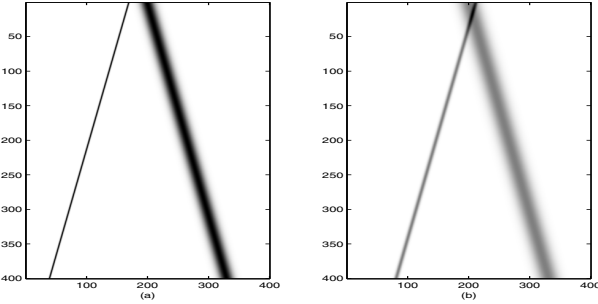

Fig. 3. Linear blurred contour retrieval: processed image (a); result (b)

Fig. 4. Fire detection: (a) initial color image; (b) Cr Channel from the image YCbCr representation; (c) processed image; (d) and (e) proposed method; (f) Chan and Vese

4.2. Circular blurred contours

We now seek for circular blurred contours: a circular antenna is adapted to the image with $S = 350$. For signal generation, a variable speed propagation scheme is chosen, with $\alpha = 2.5 \ 10^{-3}$. This value is tuned empirically, but still permits to avoid any phase indeterminacy in (7). We choose Chan and Vese [2] as a first comparative method, with a level set to 0.7, and 50 iterations. The center coordinates are estimated using the method proposed in [5]. We consider the image of Figure 4, which concerns fire front detection: fire propagates from two center points, forming two circles because the wind is not strong. We wish to localize the regions where trees are still burning, to know in advance where the fire will extend. We process the Cr channel of the YCbCr representation, which permits to get rid of the smoke (see Figure 4(b)). To fit the proposed model, a soft threshold is applied (see Figure 4(c)), based on the automatic Otsu method [11]. Results are displayed in Figures 4(d),(e),(f) including Chan and Vese approach. The estimated parameters are, for the fire on the left: center $\{l_c; m_c\} = \{70; 73\}$, radius $\hat{r} = 51.7$, and spread $\hat{\sigma} = 11.4$; on the right: center $\{l_c; m_c\} = \{169; 171\}$, radius
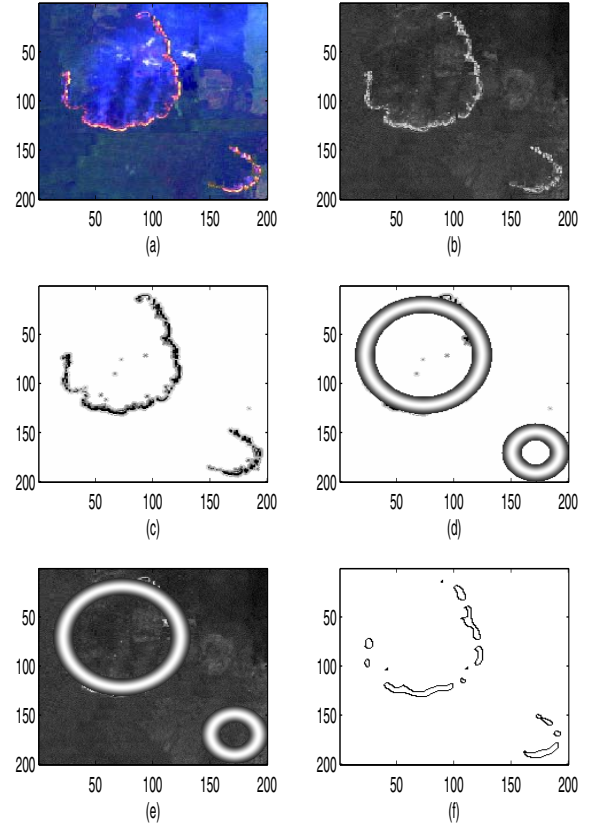
$\hat{r} = 21.4$, and spread $\hat{\sigma} = 4.2$. The radius value informs about how far the fire front progressed from the source. The spread parameter informs about the surface which is still burning.

As a second comparative method, we choose the Hough transform dedicated to circle radius estimation [12]: contrary to the Chan and Vese approach, and similarly to our approach, the Hough transform assumes the knowledge of the type of contour which is expected. In this version of the Hough transform, the circle center is supposed to be previously estimated, which is done in practice as advised in [5]. Once the center of the two fires were estimated, we applied the Hough transform: Figure 5(b) shows the superposition of the two circles obtained by the Hough transform, superimposed to the 'processed image' which is displayed in Figure 5(a). The estimated radius values are $\hat{r} = 53.8$ and $\hat{r} = 23.0$. The Hough transform yields radius values which differ by 2.1 and 1.6 from the values provided by PSO. Both methods are then robust to small variations with respect to the expected circular template. However and obviously, we notice that the spread information is lacking when the Hough transform is applied.
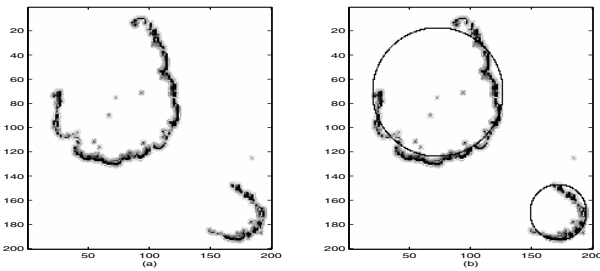
Fig. 5. Fire detection: (a) processed image; (b) Hough transform

5. CONCLUSION

An image model involving an exponential variation of grey level values, and appropriate signal generation scheme on either linear or circular antenna yields a signal model including the contour parameters. In this paper, the estimation of linear blurred contours and circular blurred contours get closer to each other: we propose a common signal model, whose components depend in a nonlinear fashion of the contour parameters. For the first time, we show that particle swarm optimization is more adequate than other optimization methods used in this field, to estimate all contour parameters. The proposed method was successfully exemplified to a hand-made image and on a remote sensing application: fire characterization.

REFERENCES

[1] H. Wang and T. Huang, "Region-based object and background extraction via active contours ",*Optik - Int. J'l for Light and Electron Optics*, vol. 124, no. 23, pp. 6020-6026, 2013.

[2] T.F. Chan and L.A. Vese, "Active contours without edges", *IEEE Trans. on Image Processing*, vol. 10, no. 2, pp. 266-277, 2001.

[3] W. Fang and K. Chan, "Incorporating shape prior into geodesic active contours for detecting partially occluded object", *Int. J. Pattern Recognition*, vol. 40, pp. 2163-2172, 2007.

[4] H. Jiang, J. Marot, C. Fossati, S. Bourennane, "Fuzzy contour characterization by subspace based methods of array processing and direct method", in *Proc. EUSIPCO'10*, Aalborg, August 2010, pp. 1344-1348.

[5] H. Jiang, J. Marot, C. Fossati, S. Bourennane, "Circular contour retrieval in real-world conditions by higher order statistics and an alternating-least squares algorithm", *Eurasip Journal on advances in signal processing*, vol. 2011, no. 1, November 2011.

[6] H. K. Aghajan and T. Kailath, "Sensor array processing techniques for super resolution multi-line-fitting and straight edge detection", *IEEE trans. on Image Processing*, vol. 2, no. 4, pp. 454-65, 1993.

[7] J. Marot and S. Bourennane, "Subspace-Based and DIRECT Algorithms for Distorted Circular Contour Estimation", *IEEE Trans. on Image Processing* vol. 16, no. 9, pp. 2369-2378, 2007.

[8] J. C. Lagarias, J. A. Reeds, M. H. Wright, and P. E. Wright, "Convergence Properties of the Nelder-Mead Simplex Method in Low Dimensions", *SIAM Journal of Optimization*, vol. 9, no. 1, pp. 112-147, 1998.

[9] D.R. Jones, C.D. Pertunen, and B.E. Stuckman, "Lipschitzian optimization without the Lipschitz constant", *J'l of Optimization theory and Application*, vol. 79, no. 1, pp. 157-181, October 1993.

[10] J. Kennedy and R. Eberhart, "Particle swarm optimization", in *Proc. IEEE International Conference on Neural Networks*, Perth, 1995, pp. 1942-1948.

[11] N. Otsu, "A threshold selection method from gray-level histograms", *IEEE Trans. Sys., Man., Cyber.*, vol. 9, no. 1, pp. 62-66, 1979.

[12] L. Jiang, "Efficient randomized Hough transform for circle detection using novel probability sampling and feature points", *Optik - International Journal for Light and Electron Optics*, vol. 123, no 20, pp. 1834-1840, 2012.